

Multiscale pulse dynamics in communication systems with strong dispersion management

Mark J. Ablowitz and Gino Biondini*

Department of Applied Mathematics, University of Colorado at Boulder, Campus Box 526, Boulder, Colorado 80309-0526

Received July 9, 1998

The evolution of an optical pulse in a strongly dispersion-managed fiber-optic communication system is studied. The pulse is decomposed into a fast phase and a slowly evolving amplitude. The fast phase is calculated exactly, and a nonlocal equation for the evolution of the amplitude is derived. In the limit of weak dispersion management the equation reduces to the nonlinear Schrödinger equation. A class of stationary solutions of this equation is obtained; they represent pulses with a Gaussian-like core and exponentially decaying oscillatory tails, and they agree with direct numerical solutions of the full system. © 1998 Optical Society of America

OCIS codes: 060.0060, 060.2310, 060.4510, 060.5530, 260.2030.

The use of asymptotic methods to describe the long-time dynamics of a physical system is an essential tool in a variety of situations. The nonlinear Schrödinger (NLS) equation, derived by asymptotic methods from Maxwell's equations, plays a central role in fiber optics in the study of long-distance communication systems. The NLS equation also appears as an average equation when one is considering perturbations such as damping–amplification and moderate dispersion management.^{1,2} In the past few years widespread interest has focused on transmission links that make substantial use of dispersion management, owing to their many remarkable features when compared with systems with constant dispersion.^{3–9} In this Letter we obtain the asymptotic equations governing pulse dynamics in such systems. By formulating an appropriate multiscale perturbation expansion, we decompose the dynamics of the pulse in the Fourier domain into the product of a rapidly varying phase and a slowly evolving amplitude. The rapid phase is completely determined by the large periodic variations of the dispersion, while the amplitude satisfies a nonlocal equation [Eqs. (5) below] that reduces to the usual NLS equation in the limit of weak dispersion management. Interestingly, the equation has dual representation in the Fourier and the temporal domains. We derive a two-parameter family of localized traveling-wave solutions. These solutions are characterized by a Gaussian-like core with exponentially decaying oscillatory tails and are consistent with direct numerical simulations of the perturbed NLS equation with dispersion management.

We start from the perturbed NLS equation

$$iu_z + (1/2)D(z)u_{tt} + |u|^2u = 0, \quad (1)$$

where all quantities are expressed in dimensionless units: t is the retarded time, z is the propagation distance (with the unit length defined in terms of the path-average dispersion), u is the slowly varying envelope of the optical field, and $D(z)$ represents the fiber dispersion. Loss and amplification can be included by a change of variables.⁴ We model strong dispersion management by splitting the dispersion $D(z)$ into two components: $D(z) = \delta_a + (1/z_a)\Delta(z/z_a)$. The variable z_a is the dispersion-map period, which is assumed to be small compared with the disper-

sion length, i.e., $z_a \ll 1$. The constant δ_a represents the small path-average dispersion, whereas $\Delta(z/z_a)$, which is periodic with zero average, describes the large, rapid variations that correspond to the local changes of the value of fiber dispersion. Here and below all averages are taken over one period of the dispersion map, z_a : $\langle f \rangle \equiv (1/z_a) \int_0^{z_a} dz f(z)$. The proportionality factor $1/z_a$ in front of $\Delta(z/z_a)$ is chosen so that both δ_a and $\Delta(z/z_a)$ are quantities of order one.

Equation (1) contains both large and rapidly varying terms. To obtain the asymptotic behavior we introduce fast and slow z scales as² $\zeta = z/z_a$ and $Z = z$, respectively, and we expand the field u in powers of z_a :

$$u(\zeta, Z, t) = u^{(0)}(\zeta, Z, t) + z_a u^{(1)}(\zeta, Z, t) + \dots \quad (2)$$

In this way Eq. (1) breaks into a series of equations corresponding to the different powers of z_a . In general, at order $O(z_a^{n-1})$ we have

$$\begin{aligned} F[u^{(n)}] &:= iu_{\zeta}^{(n)} + (1/2)\Delta(\zeta)u_{tt}^{(n)} \\ &= -P_n[u^{(0)}, u^{(1)}, \dots, u^{(n-1)}], \end{aligned} \quad (3)$$

where $P_0 = 0$, $P_1[u^{(0)}] = iu_Z^{(0)} + (1/2)\delta_a u_{tt}^{(0)} + |u^{(0)}|^2 u^{(0)} = 0$, and so on. At $O(z_a^{-1})$ we have $F[u^{(0)}] = 0$. That is, to leading order, the evolution of the pulse is determined solely by the large variations of $D(z)$ about its mean: nonlinearity and residual dispersion represent only a small perturbation to the linear solution.⁸ Employing Fourier transforms [defined as $f(t) = (1/2\pi) \int_{-\infty}^{\infty} d\omega \exp(i\omega t) \hat{f}(\omega)$], we obtain

$$\hat{u}^{(0)}(\zeta, Z, \omega) = \hat{U}(Z, \omega) \hat{p}(C(\zeta), \omega), \quad (4)$$

where $\hat{p}(x, \omega) = \exp[-(i/2)x\omega^2]$ and $C(\zeta) = C_0 + \int_0^{\zeta} d\zeta' \Delta(\zeta')$, with C_0 arbitrary. The integration constant $\hat{U}(Z, \omega)$ represents the slowly evolving amplitude of $\hat{u}^{(0)}$, whereas $\hat{p}(C(\zeta), \omega)$ contains the fast oscillations induced by the local values of the dispersion. The function $\hat{U}(Z, \omega)$ is arbitrary at this stage and needs to be determined at higher orders.

At the next-to-leading order in the expansion we have $F[u^{(1)}] = -P_1[u^{(0)}]$. Again, we use Fourier transforms to solve explicitly for $\hat{u}^{(1)}(\zeta, Z, \omega)$. To avoid secularities, we need the forcing term in the Fourier domain to be orthogonal to $\hat{p}(C(\zeta), \omega)$, i.e., $\int_0^1 d\zeta \hat{p}^*(C(\zeta), \omega) \hat{P}_1[u^{(0)}(\zeta, Z, \cdot)] = 0$. This condition determines a nonlinear evolution equation for the unknown function $\hat{U}(Z, \omega)$:

$$i\hat{U}_Z - \frac{1}{2} \delta_a \omega^2 \hat{U} + \iint_{-\infty}^{+\infty} d\omega_1 d\omega_2 \hat{U}(Z, \omega + \omega_1) \times \hat{U}(Z, \omega + \omega_2) \hat{U}^*(Z, \omega + \omega_1 + \omega_2) r(\omega_1 \omega_2) = 0, \quad (5a)$$

where the kernel $r(x)$ is given by $r(x) = 1/(2\pi)^2 \times \int_0^1 d\zeta \exp[iC(\zeta)x]$. By taking the inverse Fourier transform of Eq. (5a) we obtain the corresponding evolution equation in the time domain:

$$iU_Z + \frac{1}{2} \delta_a U_{tt} + \iint_{-\infty}^{+\infty} dt_1 dt_2 U(Z, t + t_1) \times U(Z, t + t_2) U^*(Z, t + t_1 + t_2) R(t_1, t_2) = 0, \quad (5b)$$

where $R(t_1, t_2) = \iint_{-\infty}^{+\infty} d\omega_1 d\omega_2 \exp(i\omega_1 t_1 + i\omega_2 t_2) \times r(\omega_1 \omega_2)$.

Equation (5b) is the universal asymptotic equation that governs the evolution of the amplitude of an optical pulse in a strongly dispersion-managed system described by Eq. (1). All fast and large variations have been removed. Note that Eq. (5b) is not limited to the case $\delta_a > 0$ and applies equally well to description of pulse dynamics with zero or normal values of average dispersion. If $\Delta(\zeta) = 0$ (that is, if the fiber dispersion is constant) and $C_0 = 0$, then $C(\zeta) = 0$; hence $r(x) = 1/(2\pi)^2$ and $R(t_1, t_2)$ becomes a two-dimensional Dirac delta: $R(t_1, t_2) = \delta(t_1)\delta(t_2)$. As a consequence, Eqs. (5a) and (5b) reduce to the usual NLS equation, written in the Fourier and the temporal domain, respectively. Note that Eq. (5a) is invariant under the combined transformations $r(x) \rightarrow \exp(iC_0 x)r(x)$ and $\hat{U}(Z, \omega) \rightarrow \exp(iC_0 \omega^2/2)\hat{U}(Z, \omega)$; therefore the constant C_0 appearing in $C(\zeta)$ can be chosen arbitrarily and does not affect the solution of the original problem. Equation (5b) is also invariant under Galilean transformations: if $U(Z, t)$ is a solution of Eq. (5b), then $U'(Z, t) = \exp[(i/2)(vt - v^2 Z/2)]U(Z, t - vZ)$ also satisfies Eq. (5b), for any real v . Finally, the pulse energy, defined as $\|U\|^2 = \int dt |U(Z, t)|^2$, is conserved, and two additional conserved quantities exist in the form of the momentum and the Hamiltonian.

All the calculations presented above are valid for a general dispersion map. In the special case of a piecewise constant map, the integration kernels can be calculated explicitly. For a two-step map we take $\Delta(\zeta)$ to be the periodic extension of $\Delta(\zeta) = \Delta_1$ for $0 \leq |\zeta| < \theta/2$ and $\Delta(\zeta) = \Delta_2$ for $\theta/2 \leq |\zeta| < 1/2$. Then the condition $\langle \Delta \rangle = 0$ yields $\Delta_1 \theta = -\Delta_2(1 - \theta)$. We introduce the parameter $s = [\theta \Delta_1 - (1 - \theta) \Delta_2]/4$, which provides a measure of the normalized map strength.

Then, if we fix the integration constant C_0 by requiring that the average chirp along one dispersion map be zero, we have $C_0 = 0$ and the points where $C(\zeta)$ is zero are the midpoints of each fiber segment: $\zeta = 0$ and $\zeta = 1/2$. Since $\hat{p}(0, \omega) = 1$ and $p(0, t) = \delta(t)$, at these values of ζ the solution $u^{(0)}(\zeta, Z, t)$ coincides with $U(Z, t)$. For these two-step maps the kernels $r(x)$ and $R(t_1, t_2)$ are $r(x) = \sin(sx)/[(2\pi)^2 sx]$ and $R(t_1, t_2) = (1/2\pi|s|)\text{ci}(t_1 t_2/s)$, respectively, where $\text{ci}(x) = \int_1^\infty dy \cos(xy)/y$ is the cosine integral. Note that, since $|r(x)| \leq 1/(2\pi)^2$, the strength of the coupling between different frequencies is always less than that for the ordinary NLS equation.

Next we look for traveling-wave solutions of Eq. (5b). Since this equation is invariant under Galilean transformation, traveling-wave solutions can be obtained by use of such a transformation if stationary solutions are known. Therefore we look for solutions of the form $U(Z, t) = f(t)\exp[(i/2)\lambda^2 Z]$, with $f(t)$ real and even. The Fourier transform $F(\omega)$ of $f(t)$ is also real and even. Then, using Eq. (5a), we have the following nonlinear integral equation for $F(\omega)$:

$$(\lambda^2 + \delta_a \omega^2)F(\omega) = 2 \iint_{-\infty}^{+\infty} d\omega_1 d\omega_2 F(\omega + \omega_1)F(\omega + \omega_2) \times F(\omega + \omega_1 + \omega_2)r(\omega_1 \omega_2). \quad (6)$$

By scaling arguments it can be shown that, if $F_1(\omega)$ is a solution of Eq. (6) corresponding to the eigenvalue $\lambda = \lambda_1$ and $s = s_1$, then $F_2(\omega) = F_1(\omega/\alpha)$ is also a solution, corresponding to the eigenvalue $\lambda_2 = \alpha \lambda_1$ and the map strength $s_2 = s_1/\alpha^2$. Therefore a family of solutions can be generated from the knowledge of just one. Note also that $f_2(t) = \alpha f_1(\alpha t)$, which means that the scaling parameter α is also directly proportional to the pulse energy and inversely proportional to the pulse width. That is, $\|f_2\|^2 = \alpha \|f_1\|^2$ and $\tau_2 = \tau_1/\alpha$, as for the classical NLS equation. As in Ref. 3, to get the dependence of the energy on the map strength (that is, the power-enhancement factor), one needs to go to higher orders in the perturbation expansion.

The solutions in the family described above are characterized by the same value of δ_a . Here we restrict ourselves to the case $\delta_a = 1$, and we solve Eq. (6) numerically. Figure 1(a) shows a plot of $F(\omega)$ versus ω for $s = 1$ and $\lambda = 4$. The solid curves represent the positive part of $F(\omega)$, and the dotted-dashed curves represent the negative part. The dashed curve represents a sech pulse with the same FWHM in the frequency domain. Figure 1(b) shows the corresponding plot of $f(t)$ versus t . Again, the solid curve represents the positive part and the dotted-dashed curves represent the negative part (in contrast, the familiar soliton solutions of the NLS equation are always positive in both the time and the frequency domains), and the dashed curve is a sech pulse with the same FWHM in the temporal domain. The agreement of these pulses with numerical solutions of Eq. (1) with strong dispersion management (cf. Fig. 1 in Ref. 6) is remarkable. The main features of the new pulses are a Gaussian-like center and exponentially decaying

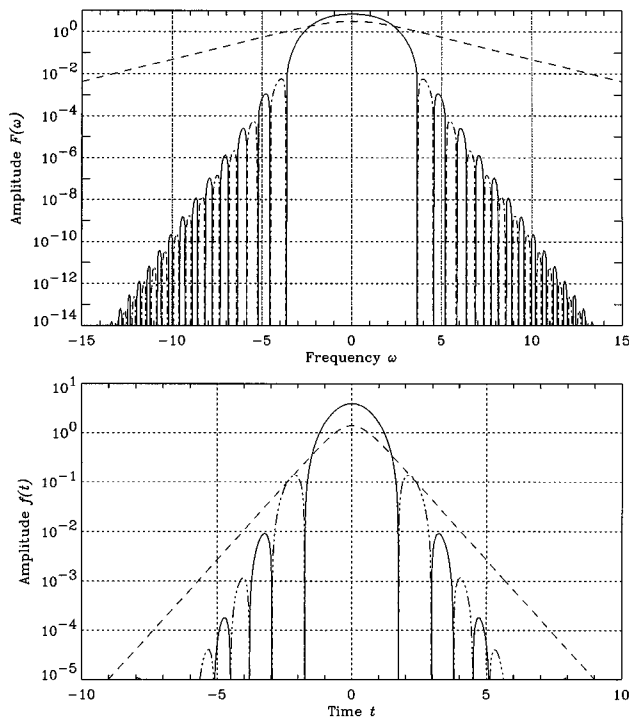


Fig. 1. Shape of the stationary pulses in the Fourier and temporal domains for $s = 1$ and $\lambda = 4$.

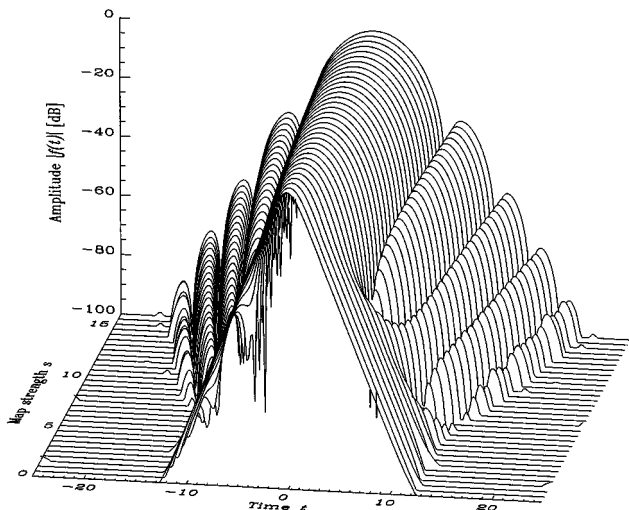


Fig. 2. Shape of the stationary pulses in the temporal domain for $\lambda = 1$ and various values of s .

tails, characterized by oscillations with a frequency that increases with increasing distance from the center of the pulse. Note also that the energy of the pulse is more concentrated in the center than for NLS pulses with the same FWHM. Figure 2 illustrates the profiles of $f(t)$ for a sequence of different values of s from 0 to 16, for a fixed value of $\lambda = 1$. By virtue of the scaling symmetry mentioned above, the plot also represents a class of solutions corresponding to a fixed

value of s and varying values of λ . We should mention that Eq. (6) can also be used to look for stationary solutions in the zero or the normal average dispersion regime, i.e., when $\delta_a \leq 0$. In fact, we already obtained such solutions, which possess the same structure.

From $F(\omega)$, using Eq. (4), we can reconstruct the evolution of the solution with z . The result is a breathing pulse that shows a remarkable correspondence with direct simulations of Eq. (1) (Fig. 2 in Ref. 6). Since $f(t)$ is real and even, and since $C(\zeta)$ is symmetrical with respect to the fiber midpoints, the values of $u^{(0)}(\zeta, Z, t)$ at the fiber endpoints are the complex conjugate of each other. We further tested our model by integrating Eq. (1) numerically. As z_a is decreased, the breathing solutions of Eq. (1) rapidly converge to the solutions obtained from our average equation. In particular, the convergence rate is linear in z_a , and with $z_a = 0.01$ the difference between solutions of Eq. (5b) and of Eq. (1) is less than 3×10^{-3} of the maximum pulse amplitude. The slight disagreement between the two models depends on the high-order corrections to the leading-order solution, which are also responsible for the difference between the pulse profiles taken at the fiber midpoints.

A number of problems remain to be discussed, including a detailed study of the properties of the averaged nonlocal equation (such as symmetries and conservation laws), a complete characterization of the stationary solutions (including the case of normal average dispersion), the role of higher-order corrections, pulse interactions, wavelength-division multiplexing, and the effects of damping–amplification.

We acknowledge many valuable discussions with W. L. Kath. This effort was partially sponsored by the U.S. Air Force Office of Scientific Research, Air Force Materials Command, U.S. Air Force, under grant F49620-97-1-0017.

*E-mail address biondini@colorado.edu.

References

1. A. Hasegawa and Y. Kodama, *Opt. Lett.* **15**, 1443 (1990); *Opt. Lett.* **16**, 1385 (1991); I. R. Gabitov and S. K. Turitsyn, *Opt. Lett.* **21**, 327 (1996).
2. T.-S. Yang and W. L. Kath, *Opt. Lett.* **22**, 985 (1997).
3. Y. Kodama, S. Kumar, and A. Maruta, *Opt. Lett.* **22**, 1689 (1997).
4. T.-S. Yang, W. L. Kath, and S. K. Turitsyn, *Opt. Lett.* **23**, 597 (1998).
5. N. J. Smith, N. J. Doran, F. M. Knox, and W. Forysiak, *Opt. Lett.* **21**, 1981 (1996).
6. J. H. B. Nijhof, N. J. Doran, W. Forysiak, and F. M. Knox, *Electron. Lett.* **33**, 1726 (1997).
7. J. N. Kutz and S. G. Evangelides, *Opt. Lett.* **23**, 685 (1998); J. N. Kutz, P. Holmes, S. G. Evangelides, and J. P. Gordon, *J. Opt. Soc. Am. B* **15**, 87 (1998); V. S. Grigoryan and C. R. Menyuk, *Opt. Lett.* **23**, 609 (1998).
8. S. K. Turitsyn, *Sov. Phys. JETP Lett.* **65**, 845 (1997).
9. I. R. Gabitov, E. G. Shapiro, and S. K. Turitsyn, *Opt. Commun.* **134**, 31 (1997); S. K. Turitsyn and E. G. Shapiro, *Opt. Lett.* **23**, 682 (1998).